Contributions of the Ionic Lattice, Nonangular Substituents, and Perfluoroaromatic π-Stacking to the Solid States of Derivatives of *N*-Benzyl-2-phenylpyridinium Bromide

Christopher B. Martin, Brian O. Patrick,† and Arthur Cammers-Goodwin*

University of Kentucky, Department of Chemistry, Lexington, Kentucky 40506

Received May 7, 1999

A study of the crystal packing of six derivatives of *N*-benzyl-2-phenylpyridinium bromide demonstrated the potential importance of synergism between π-stacking interactions and steric substituent effects in the determination of molecular orientations in an ionic lattice. *N*-Benzyl-2-phenylpyridinium bromide was substituted with 4-methoxybenzyl, 4-cyanobenzyl, 4-trifluoromethylbenzyl, 4-trifluoromethyl-2,3,5,6-tetrafluorobenzyl, and 2,3,4,5,6-pentafluorobenzyl. Nonangular para substituents on the benzyl ring gave rise to predictable changes in the solid state. These substituents anchored and aligned the molecules by complete or partial interdigitation. The increased stability of perfluoroarene/arene interactions vs arene/arene interactions were manifest in the presence of the strong ionic lattice. The fact that electronic perturbation in π-stacked oriented molecules in these crystals demonstrated partial orthogonality between the directional forces involved in the establishment of the ionic lattice and the much weaker directional contributions to the lattice energy from π-stacking.

Introduction

Conduction[1,2] and nonlinear optical properties[3] of organic solids often depend on molecular order and contact between π-conjugated systems. Due to the importance of molecular orientation on bulk properties of crystalline solids, experimentalists[4−10] and theoreticians[11] have applied their talents toward the design and prediction of the solid state of organic compounds. Despite the effort, predicting the molecular disposition of the organic solid state is still an elusive goal.[12] Organic crystal engineering relies on nature's usual arsenal of intermolecular forces: electrostatic, hydrogen bonding,[13] dipolar, molecular orbital interaction,[14] van der Waals dispersion,[15] and quadrupolar.[16] Also, chemists often cite π-stacking, a relatively weak interaction, in the orientation of molecules in the solid state.[17]

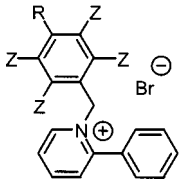

Figure 1. 1: R,Z = H; **2**: R = OMe, Z = H; **3**: R = CN, Z = H; **4**: R = CF_3, Z = H; **5**: R = CF_3, Z = F; **6**: R, Z = F.

The previous accompanying paper[20] explored intramolecular π-stacking of the title compounds in the solution and solid states. In this study, we show that the strong ionic lattice of **1**−**6** (Figure 1) determined the crystal packing to a first approximation. This fact was in question because Br(−) is large and the pyridinium cations are delocalized. To a second approximation, two much weaker interactions determined the molecular disposition of these crystal structures in the presence of the ionic lattice. (1) A nonangular *p*-benzyl substituent of sufficient size impeded intermolecular π-stacking and aligned molecules with respect to the ionic planes in the crystals. (2) The known preference for face-to-face (FF) π-stacking in perfluoroarene/arene interactions emerged when benzyl was substituted with pentafluorobenzyl in the absence of a nonangular para substituent.

Results and Discussion

Alternating Ionic and Hydrocarbon Layers. The solid states of **1**−**6** alternated double layers of hydrocarbon and ionic substructures. The ionic substructure is taken to be the pyridinium bromide portion of the molecule, and the hydrocarbon terminus is defined as the Bn and Ph substituents. This alternating motif is obvious in Figures 3−8. To investigate the contribution of the

† University of Kentucky Department of Chemistry X-ray Crystallography Laboratory.

(1) Geiser, U.; Schlueter, J. A.; Wang, H. H.; Kini, A. M.; Williams, J. M.; Sche, P. P.; Zakowiz, H. I.; VanZile, M. I.; Dudek, J. D.; Nixon, P. G.; Winter, R. W.; Gard, G. L.; Ren, J.; Whangbo, M.-H. *J. Am. Chem. Soc.* **1996**, *118*, 9996−9997.
(2) Miller, L.; Mann, K. R. *Acc. Chem. Res.* **1996**, *29*, 417−423.
(3) Thalladi, V. R.; Brasselet, S.; Weiss, H.-C.; Blaser, D.; Katz, A. K.; Carrell, H. L.; Boese, R.; Zyss, J.; Nangia, A.; Desiraju, G. R. *J. Am. Chem. Soc.* **1998**, *120*, 2563−2577.
(4) Zimmerman, S. C. *Science* **1997**, *276*, 543−544.
(5) Gavezzotti, A. *Acc. Chem. Res.* **1994**, *27*, 309.
(6) Desiraju, G. R. *Science* **1997**, *278*, 404.
(7) Braga, D.; Grepioni, F.; Desiraju, G. R. *Chem. Rev.* **1998**, *98*, 1375.
(8) Aakeröy, C. B. *Acta Crystallogr., Sect. B* **1997**, *53*, 4.
(9) Nangia, A.; Desiraju, G. R. *Top. Curr. Chem.* **1998**, *198*, 58−95.
(10) Caira, M. R. *Top. Curr. Chem.* **1998**, *198*, 164−208.
(11) Lii, J.-H.; Allinger, N. L. *J. Am. Chem. Soc.* **1989**, *111*, 8576−8582.
(12) Wolff, J. J. *Angew. Chem., Int. Ed. Engl.* **1996**, *35*, 2195.
(13) Brasselet, S.; Desiraju, G. R.; Campbell, J. P.; Hwang, J.-W.; Gladfelter, W. L. *J. Am. Chem. Soc.* **1998**, *120*, 2563.
(14) Greer, M. L.; McGee, B. J.; Blackstock, S. C. *Angew. Chem., Int. Ed. Engl.* **1997**, *36*, 1864.
(15) Reddy, D. S.; Craig, D. C.; Desiraju, G. R. *J. Am. Chem. Soc* **1996**, *118*, 4090−4093.
(16) Williams, J. H. *Acc. Chem. Res.* **1993**, *26*, 593−598.
(17) Hunter, C. A.; Sanders, J. K. M. *J. Am. Chem. Soc.* **1990**, *112*, 5525−5534.

10.1021/jo990765t CCC: $18.00
Published on Web 09/21/1999

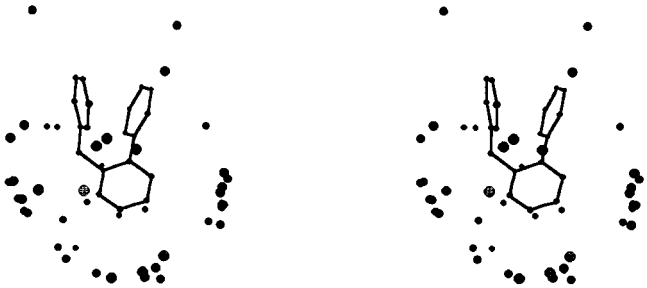

Figure 2. Distribution of Br atoms around the pyridinium substructure.

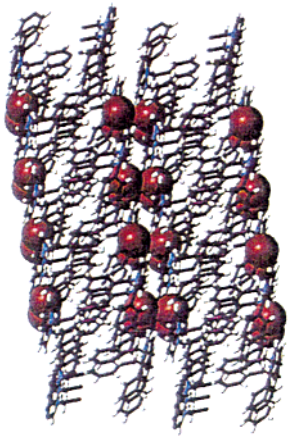

Figure 3. Figures 3−8 show that the solid states of **1**−**6** are analogous. In Figures 4−8, the hydrogen atoms were removed for clarity. All the figures show analogous perspectives of the ionic and hydrocarbon alternating double-layer motif.

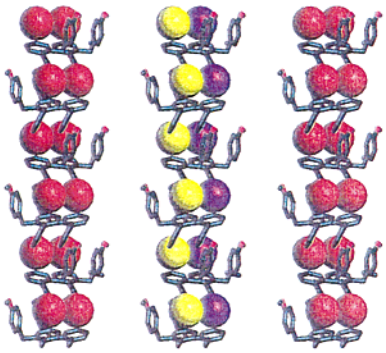

Figure 4. Compound **2**, with Br(−) atoms in CPK. One layer of one double layer is colored yellow and the other layer purple. The yellow spheres are coplanar, but not collinear.

ionic lattice to the solid-state motif, delocalization of the positive charge in these pyridinium derivatives was explored with calculations. The pyridinium ring and the *N*-methylene bore 76.3, 74.5, 79.1, and 87.4% of the total positive charge in **1**, **2**, **5**, and **6**, respectively. Mulliken distribution of charges on the protons were summed into the heavy atoms at the 3-21G level of theory.

The Cambridge Crystal Structure Database (CSD)[18] was surveyed for pyridinium possessing one carbon atom on N and one carbon atom on C2 of the pyridinium ring. The CSD contained three structures with Br(−) as the

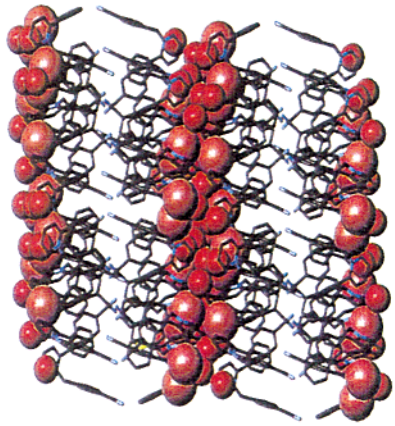

Figure 5. Comound **3** with waters of inclusion as discussed in the text.

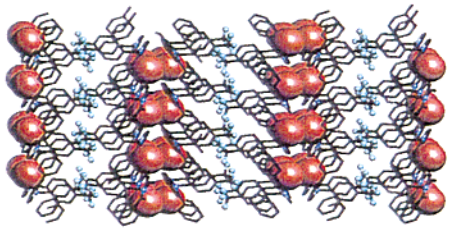

Figure 6. See Figure 3 caption.

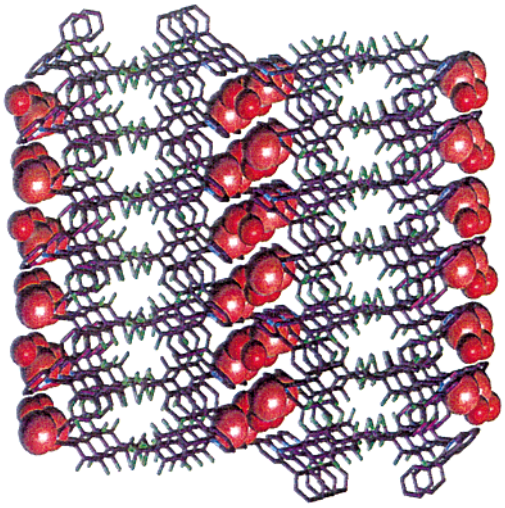

Figure 7. Compound **5** with waters of inclusion as discussed in the text.

counterion that fit the criteria.[19] Spheres of inclusion were centered at each unique Br atom in **1**−**6** and in the three structures found in the CSD. The first shell of molecules surrounding each unique Br(−) was isolated with the accompanying Br atom. Typically, this search technique found three to six ion pairs for every unique Br(−) ion in each crystal structure. The ion pairs were overlain at C2, C4, and C6 of the pyridinium ring while conserving the spatial relationships of each ion pair. Figure 2 shows the conformation of **1** in the solid state with all aforementioned ion-pair spatial relationships. Clustering of Br(−) atoms around the py(+) indicated

(18) 3D Search and Research Using the Cambridge Structural Database, Oct 98 release, version 5.16. Allen, F. H. a. K., O. *Chem. Design Automation News* **1993**, **8**, 31−37.

(19) CSD codes: BAZPUN, MPYINB10, and PAMVAA.

(20) Martin, C. B.; Mulla, H. R.; Willis, P. G.; Cammers-Goodwin, A. *J. Org. Chem.* **1999**, *64*, 7802.

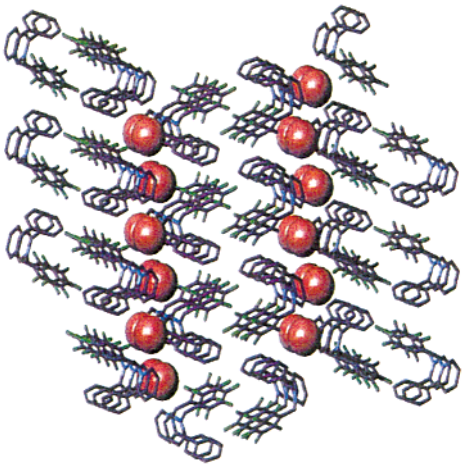

Figure 8. See Figure 3 caption.

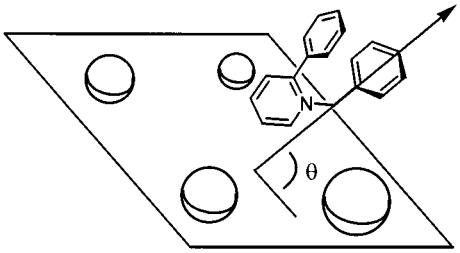

Figure 9. Graphical definition of θ. The coplanar spheres represent bromide ions. Only interactions between para-substituted benzyl groups on the all-carbon termini resulted in the ladder-like motif achieved when $\theta \approx 90°$.

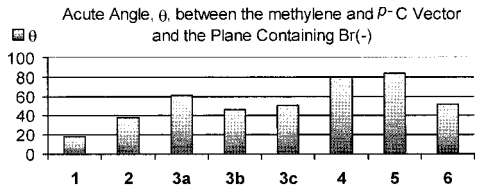

Figure 10. θ in Figure 9 as a function of benzyl derivative. The nonangular para-substituted derivatives were nearly orthogonal to the plane containing Br(−). There were three unique molecules in the solid state of **3**; these are labeled **a**, **b** and **c**.

that the ionic lattice was a strong directional force in the determination of the solid state. Note that Figure 2 does not depict specific ion pairs, but rather the spatial relationships between Br(−) and the proximal organic cations. The crystal structures of **5** and **3** were successfully solved with the inclusion of one molecule of water in **5** and three molecules of water in **3**. Water molecules in **3** and **5** associated closely with Br(−) and did not perturb the disposition of the molecules in the solid state. For example, the solid states of **4** and **5** pack in a nearly isomorphic manner (see Figures 6 and 7) and **4** lacked waters of inclusion.

The packing diagrams in **3**−**8** appear ladder-like due to alignment of the organic cations. The bar graph in Figure 10 quantifies differences in the alignment of the organic structures and gives clues about the source of the molecular alignment. The line containing the vector defined by the $-CH_2-$ and *p*-carbon atom of the *N*-benzyl substituent intersected the double plane containing Br atoms; see Figure 9. The acute angle of intersection, θ, was taken to be an expression of the molecular alignment

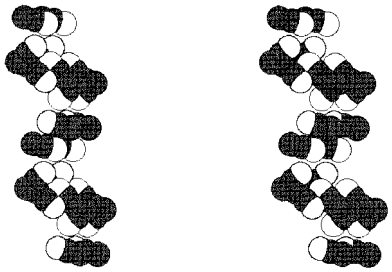

Figure 11. *p*-C atom and the *p*-CN packing arrangement in **3**.

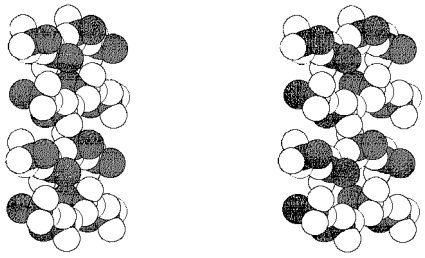

Figure 12. Fragments of the benzyl *p*-C atom and the *p*-CF_3 group showing the packing arrangement in **4**. Note that the CF_3 substituents slipped passed each other at the hydrocarbon junction.

with respect to the ionic plane. The solid state of **3** had three unique conformations, and these were labled **3a**−**c**. It is interesting that **4** and **5** are nearly normal to the ionic plane, whereas the other θ deviated significantly from 90°. Common structural features between these two solid states promoted orthogonality between the hydrocarbon portions of the molecules and the ionic plane.

Driven by Coulombic forces from the ionic lattice, the molecules butt firmly together at the phenyl and benzyl substructures. Whether or not the derivatives of **1** π-stacked or aligned themselves with respect to the plane containing Br(−) or Br(−)/H_2O was contingent on the molecules overlapping or interlocking at the hydrocarbon termini. When the molecules made good contact, θ in Figure 9 approached 90° and intermolecular π-stacking was minimal. The molecule can optimize *intramolecular* π-stacking under these conditions.

Interlocking discussed above was facilitated by certain substituents. The common factor between structures **3**−**5** was the nonangular para substituent on the benzyl ring. If the substituents filled the voids created when the aromatic rings butted together, then the acute angle, θ, in Figure 9 approached 90°. Trifluoromethyl groups filled the voids well. Arrays of fragments composed of the *p*-benzyl C atom and the *p*-substituent from the solid states of **3**, **4**, and **5** are depicted in Figures 11−13. The trifluoromethyl substituents in **4** extensively interdigitated. Interactions between the CF_3 substituents in **5** were similar to those in **4**; however, the CF_3 substituents in **5** did not slip by each other and interlock in the same manner as in **4**. Closer examination of the packing diagrams revealed the reason. The F atoms ortho to the CF_3 groups on the benzyl rings in **5** blocked interdigitation of CF_3 substituents. Lack of interdigitation in the *p*-Bn substituents of **5** probably gave rise to more disorder in the CF_3 substituents than was present in **4**. Disorder in the CF_3 substituent in **5** was modeled with all C−F bonds restrained to the same length. The populations of each fragment were determined by adjusting the oc-

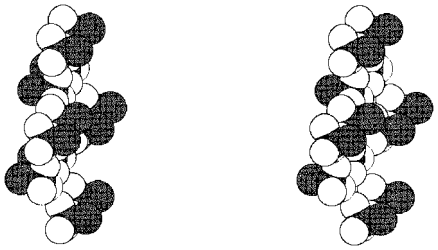

Figure 13. Fragments of the benzyl *p*-C atom and the *p*-CF_3 group showing the packing arrangement in **5**. The CF_3 substituents are almost coplanar at the hydrocarbon junction.

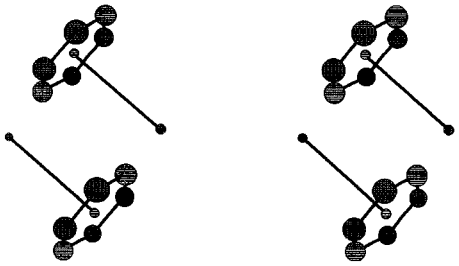

Figure 14. Stereoview of the spatial relationship between two benzyl rings in **1** that butt together in the hydrocarbon cluster. The figure contains lines normal to the plane of the aromatic rings. The operational definition of π-stacking was not met by the interaction shown for **1** because the normal lines of neither ring pierced the van der Waals radius of the carbon atoms of the corresponding ring.

cupancies until the F atoms in each fragment had roughly equivalent temperature factors. The final occupancies of the major and minor fragments were found to be 0.55 and 0.45, respectively.

Solid states **1**, **2**, and **6** did not crystallize in the rung-and-ladder motif observed in **4** and **5**, although alternating layers of hydrocarbon and ionic regions were observed in all solid states. The methoxy substituent in **2** was spatially incompatible with the requisite rung-and-ladder assembly observed in **4** and **5**. The *p*-cyano substituent in **3** was too small to function optimally as a rung in the rung-and-ladder motif observed in **4** and **5**. Compound **3** has far and close interactions between neighboring cyano substituents. Steric incompatibility between the small size of the CN substituent and the minimal space created when molecules of **3** packed resulted in more options in the packing diagram of **3** than in the solid states of **4** and **5**. However, solid state **3** has vestiges of the rung-and-ladder motif observed in **4** and **5**. There were three unique molecules in **3**, **3a**, **3b**, and **3c**. The third and fourth largest θ in Figure 10 were found in **3**. While the work was in progress, the importance of the nonangular substituent in the para position was realized. The partially aligned solid state of **3** and increased π-stacking interactions (over **4** and **5**) were predicted based on the solid states of **1** and **4**−**6**. The decision to put forth a steric argument was made after the solid states of **1**−**6** were carefully examined for intermolecular nonconventional hydrogen bonds; none were found.

Compound **6** lacked nonangular groups in the para position of the benzyl substituent. The well-separated, layered motif in **3**−**5** was also observed in the solid state of **6** although the motif was pleated instead of planar (see Figure 8). Since F atoms in the para positions did not project away from the aromatic ring far enough to function as a rung in the rung-and-ladder motif observed

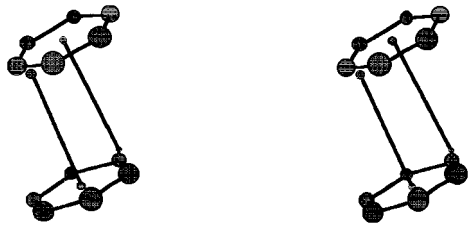

Figure 15. Stereoview of the spatial relationship between the *N*-benzyl rings in **3b** and **3c**.

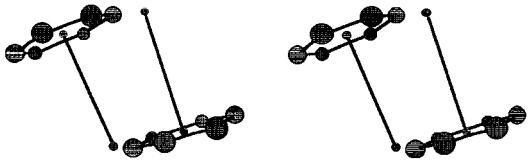

Figure 16. Stereoview of the intermolecular spatial relationship between the *N*-benzyl rings and the 2-phenyl rings in **6**.

in **3**−**5**, there must have been another mechanism responsible for the alignment of the molecules observed in the solid state of **6**.

Intermolecular face-to-face (FF) interactions were found in **1**, **3**, and **6** and were not found or were distal in the other solid states. Furthermore, the perfluoro benzyl rings in **6** intermolecularly stacked in the face-to-face, center-to-edge (FFCE) motif on the 2-phenyl substituent instead of benzyl-to-benzyl as in **1** and **3**. For the operational definition of π-stacking used in this paper see the previous paper in this issue. The *x*, *z*, and α parameters, respectively, for *intermolecular* aromatic interactions in **1**, **3,** and **6** were 3.13 Å, 3.19 Å, and 1.4°; 1.57 Å, 3.43 Å, and 3.93°; and 1.84 Å, 3.54 Å, and 16.0°.

For canonically ideal FFCE interactions, the *x* parameter should be 1.4−2.7 Å; *z* should be 3.3−4.0 Å, and α should be <45°. The interaction in **3** in Figure 15 was an ideal FFCE interaction. Large *x* parameters are tolerable for optimal π-stacking if α reorients the face of ring 2 back to the edge of ring 1 as in the solid state of **6** in Figure 16. The parameter *x* was too large in the intermolecular arene interaction in **1** in Figure 14. Instead of FF or edge-to-face (EF) stacking, these interactions appeared to be edge-to-edge or not stacked. The reason the intermolecular interaction in **1** was included in this data set was because it included two carbon atoms within 3.8 Å of at least one carbon atom in another aromatic ring. This criterion was designed to select EF interactions as well. When these criteria were met, two EF interactions were found one each in **3** and **5**. Interactions between the Bn rings in **5** were entirely EF. However, the C−C distances between the rings were long, even when the difference in the C−F versus the C−H bond length was considered.

Conclusion

This paper considered intermolecular π-stacking in derivatives of *N*-benzyl-2-phenylpyridinium bromide from the standpoint of crystal engineering. These studies indicated that the ionic lattice was the major structural element in the establishment of the solid states and probably was responsible for the alternating double-layer motif in **1**−**6**. However, the directionality of the molecular forces that gave rise to the ionic lattice was at least

Table 1. Crystal Structure Parameters for 1−3

compd	**1**	**2**	**3**
formula	$C_{18}H_{16}BrN$	$C_{19}H_{18}BrNO$	$C_{19}H_{15}BrN_2(H_2O)_{4/3}$
formula wt	326.23	356.25	374.92
cryst syst	monoclinic	monoclinic	triclinic
space grp	*P*2(1)/*c*	*P*2(1)/*c*	*P*-1
a (Å)	12.283(2)	9.235(2)	10.1497(5)
b (Å)	10.173(2)	12.680(3)	14.8513(7)
c (Å)	12.207(2)	14.995(3)	18.7305(9)
α (deg)	90.00	90.00	83.650(10)
β (deg)	101.42(3)	107.83(3)	88.690(10)
γ (deg)	90.00	90.00	73.100(10)
V (Å^3)	1495.1(5)	1671.6(6)	2684.7(2)
Z	4	4	6
D(calcd) (Mg/m^3)	1.449	1.416	1.388
T (K)	293(2)	293(2)	293(2)
cryst size (mm^3)	0.26 × 0.21 × 0.13	0.60 × 0.58 × 0.47	0.53 × 0.16 × 0.13
color, habit	colorless, transparent	colorless, transparent	colorless, transparent
F(000)	664	728	1140
abs coeff (mm^{-1})	2.739	2.460	2.304
θ data collectn range	2.62−27.88	4.45−27.88	3.77−25.06
reflns collected	6572	6654	9436
ind reflns	3535 [*R*(int) = 0.0224]	3817 [*R*(int) = 0.0285]	9436 [*R*(int) = 0.0000]
data/restraints/params	3535/0/182	3817/0 /200	9433/0/632
R_1	0.0321	0.0339	0.0511
R_{all}	0.0558	0.0437	0.0761
goodness of fit on F^2	0.976	1.023	1.067
largest diff peak and hole (e·A^{-3})	0.253 and −0.260	0.248 and −0.391	0.485 and −0.448

Table 2. Crystal Structure Parameters for 4−6

compd	**4**	**5**	**6**
formula	$C_{19}H_{15}Br\ F_3\ N$	$C_{19}H_{11}Br\ F_7N(H_2O)$	$C_{18}H_{11}BrF_5N$
formula wt	394.23	484.21	416.19
cryst syst	orthorhombic	orthorhombic	orthorhombic
space grp	*Pbca*	*Pbca*	*P*2(1)2(1)2(1)
a (Å)	10.0327(5)	10.777(2)	6.5220(10)
b (Å)	11.5311(6)	9.074(2)	8.247(2)
c (Å)	30.919(2)	39.287(8)	30.366
α (deg)	90.00	90.00	90.00
β (deg)	90.00	90.00	90.00
γ (deg)	90.00	90.00	90.00
V (Å^3)	3577.0(3)	3841.9(13)	1633.3(6)
Z	8	8	4
D (calcd) (Mg/m^3)	1.464	1.674	1.693
T (K)	173(2)	293(2)	293(2)
cryst size (mm^3)	0.46 × 0.32 × 0.18	0.32 × 0.26 × 0.16	0.395 × 0.105 × 0.063
color, habit	lt brown, transparent	colorless, transparent	colorless, transparent
F(000)	1584	1920	824
abs coeff (mm^{-1})	2.326	2.215	2.569
θ data collection range	2.42−25.00	2.07−27.79	2.56−27.84
reflns collected	9521	20258	10033
ind reflns	3073 [*R*(int) = 0.0597]	4495 [*R*(int) = 0.0594]	3832 [*R*(int) = 0.0584]
data/restraints/params	3053/6/247	4495/15/293	3832/0/218
R_1	0.0508	0.0509	0.0474
R_{all}	0.0641	0.0894	0.0767
goodness of fit on F^2	1.078	1.334	1.197
largest diff peak and hole (e·A^{-3})	0.661 and −0.653	0.593 and −0.602	0.367 and −0.383

partially orthogonal to packing forces engendered by para substitution on the benzyl group and intermolecular FF *π*-stacking. Large nonangular para substituents aligned the molecules in the solid state and appeared to segregate the aromatic rings and impede *π*-stacking. Stacking was restored in the absence of the para substituent (**1** and **6**) and with a small nonangular para substituent (**3**). *N*-*p*-Methoxybenzyl bore an angular substituent that could not fit into the spaces created when the aromatic rings butted against each other. Thus, **2** forfeited both the rung-and-ladder motif and intermolecular *π*-stacking. Compounds **4** and **5** spatially separated ionic and hydrophobic moieties most effectively due to the alignment derived from the nonangular *p*-substituent effect; compound **2** was least effective in this regard. The solid state of **5** contained loose, infinite EF stacking motifs between the benzyl fragments while **4** does not appear to intermolecularly stack.

All FF interactions were between benzyl substituents except the *N*-pentafluorobenzyl derivative, **6**. The FF affinity of perfluorobenzene for benzene appeared to manifest itself in the presence of the ionic lattice in the solid state of **6**. Herein the *N*-perfluorobenzyl substituent associated with the 2-phenyl substituent, establishing an infinite perfluorophenyl/phenyl FFCE motif. This and other observations reported in this paper were counterintuitive because relatively small perturbations on the benzyl rings resulted in similar conformations that showed notable, heuristic changes in intermolecular associations in the solid state in the presence of a strong ionic lattice. These perturbations give rise to interactions that are much weaker than the Coulombic interactions

in the ionic lattice at crystal packing distances. Hopefully, the results of this work can be incorporated into future crystal engineering of aromatic salts.

Experimental Section

Data for X-ray crystallographic analysis of compounds **1**−**6** were collected at room temperature on a Nonius KappaCCD diffractometer. Conditions used to crystallize **1**−**6** were reported in the preceding paper in this issue. Crystal structure parameters are presented in Tables 1 and 2 above.

Acknowledgment. A.C.-G. thanks the NSF (CHE-9702287) for support of this work.

Supporting Information Available: Synthesis and characterization data for all new compounds and the solid-state structures are available. This material is available free of charge via the Internet at http://pubs.acs.org.

JO990765T